

# Topology of Central Pattern Generators: Selection by Chaotic Neurons

R. Huerta, P. Varona

Institute for Nonlinear Science  
E.T.S. de Ingeniería Informática,  
Universidad Autónoma de Madrid, 28049 Madrid (SPAIN).  
huerta@routh.ucsd.edu, pvarona@lyapunov.ucsd.edu

M. I. Rabinovich

Institute for Nonlinear Science  
rabin@landau.ucsd.edu

and

Henry D. I. Abarbanel<sup>1</sup>

Department of Physics and Marine Physical Laboratory,  
Scripps Institution of Oceanography,  
hdia@jacobi.ucsd.edu

University of California, San Diego  
La Jolla CA 92093-0402 USA

arXiv:chao-dyn/9910019v1 13 Oct 1999

---

<sup>1</sup>Institute for Nonlinear Science

## Abstract

Central Pattern Generators (CPGs) in invertebrates are comprised of networks of neurons in which every neuron has reciprocal connections to other members of the CPG. This is a “closed” network topology. An “open” topology, where one or more neurons receives input but does not send output to other member neurons, is not found in these CPGs. In this paper we investigate a possible reason for this topological structure using the ability to perform a biological functional task as a measure of the efficacy of the network. When the CPG is composed of model neurons which exhibit regular membrane voltage oscillations, open topologies are essentially as able to maximize this functionality as closed topologies. When we replace these models by neurons which exhibit chaotic membrane voltage oscillations, the functional criterion selects closed topologies when the demands of the task are increased, and these are the topologies observed in known CPG networks. As isolated neurons from invertebrate CPGs are known in some cases to undergo chaotic oscillations [Hayashi & Ishizuka, 1992, Abarbanel et al 1996] this provides a biological basis for understanding the class of closed network topologies we observe.

# 1 Introduction

Central Pattern Generator (CPG) neural networks in invertebrates perform a wide variety of functional roles, each of them requiring rhythmic output from the CPG to the muscles controlling the function [Marder & Calabrese 1996]. In our study of the pyloric CPG of the California spiny lobster *Panrulis interruptus* we have addressed the question why the network is closed in the sense that all neurons in the CPG both send signals to other neurons in the circuit and receive input from other neurons in the circuit. None of the neurons only receive from or send signals to the rest of the network. The pyloric CPG is illustrated in the right half of Figure 1A.

In this paper we address the appearance of this closed CPG network and seek a functional biological reason why evolution may have been led to select this configuration. We are aware of investigations [Getting 1989] which attempt to answer this question in terms of enhancing robustness or self-organization. In the present work we test an alternate hypothesis: *the closed network topology composed of irregular neurons provides greater efficiency in the task which the network is required to perform*. We present here evidence for this hypothesis in terms of calculations of the ability of a model crustacean pyloric CPG to perform its task of transporting shredded food from the stomach to the digestive system. We build the CPG first from conductance based Hodgkin-Huxley (HH) [Hodgkin & Huxley, 1952, Huerta 1996] neurons which exhibit periodic oscillations and subsequently from model neurons of Hindmarsh-Rose (HR) [Hindmarsh & Rose, 1984] type which have chaotic membrane voltage oscillations. Using the transport criterion made explicit below, we find the periodic HH neurons to allow open topologies in CPG operation while chaotic component neurons allow only closed topologies on our functional criterion.

In an earlier paper [Huerta et al, in press] we described in some detail the use of regular HH neurons with two spatial compartments as CPG network components. Many of the allowed network configurations, were open and quite robust in the presence of noise as the HH models oscillated in a strongly dissipative limit cycle and did not sit in parameter space near a bifurcation point. In real biological networks the component neurons show substantial irregularity in their bursting cycles [Elson et al 1999, Elson et al 1998], and this has led us to the work reported here.

The chaotic model neuron we use in our investigations is a three dimensional version of an HR neuron. It exhibits spiking-bursting behavior as observed in the laboratory, and this alone would not distinguish it from similar behavior of HH type neuron models. Some evidence, peripheral to this study, for the realistic structure of the HR neurons comes from its observed ability to act as a substitute for biological neurons in the lobster pyloric CPG when it is realized in simple analog

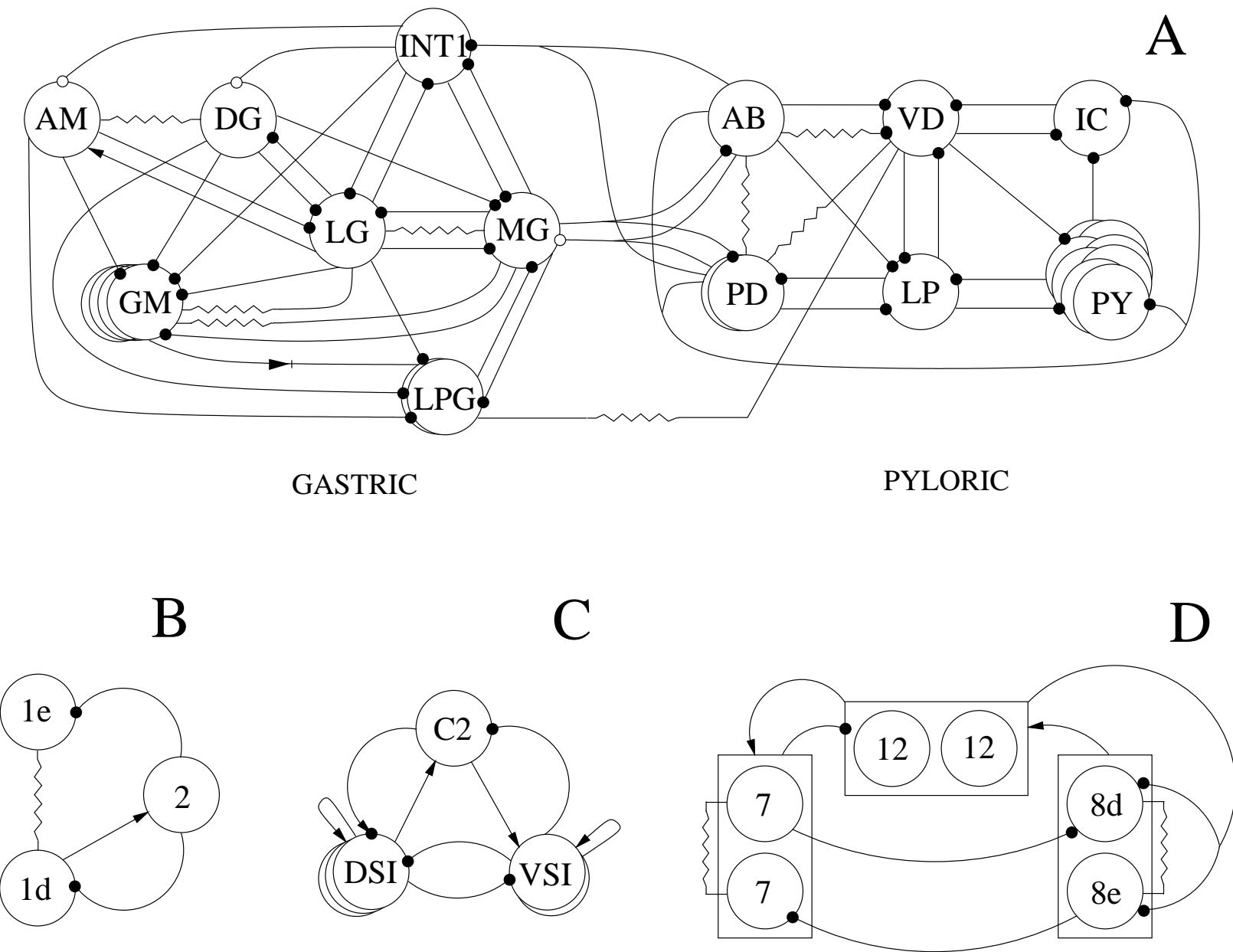


Figure 1: Examples of closed topologies in invertebrate CPGs: (A) the gastric and pyloric CPGs in crustacea (modified from [Selverston & Moulins 1987]), (B) The feeding CPG in *Planorbis* (modified from [Arshavsky et al 1985]), (C) The swimming CPG in *Tritonia* (modified from [Getting 1989]), (D) The swimming CPG in *Clione* (modified from [Arshavsky et al 1991]). Dots represent inhibitory synapses while arrows represent excitatory synapses. Electrotonic gap junctions are represented by resistors.

circuitry and coupled into that biological network [Szucs et al 1999]. The main feature of the chaotic neuron is that it is built around a homoclinic loop, which carries the fast oscillations. Motion on the homoclinic loop is intrinsically unstable which means that any perturbation close to the homoclinic

structure will produce striking differences in its membrane voltage time course: the neuron will either fire another spike or hyperpolarize the membrane [Bazhenov et al 1998, Abarbanel et al 1996, Wang 1993]. The dynamical pictures of the chaotic and the regular models are completely different.

The functional criterion we investigate is based on the role of the pyloric CPG in the California spiny lobster. The pyloric CPG has as its task the transport of shredded food from the stomach to the digestive system. Our functional criterion for the selection of network topologies is the ability to perform this transport as the severity of the task is increased. In an intuitive way one might expect to maximize this transport through regular CPG oscillations, and this is consistent with a fully coupled or closed topology of interconnections which regularize the chaotic behavior of individual components of the CPG assembly [Bazhenov et al 1998]. Our overall picture then suggests a correspondence between the functional task of a CPG, the observations of regular patterned behavior in CPG assemblies of individually chaotic components, and the CPG network topology.

## 2 The chaotic model neuron

In our simulations we used a modified, three dimensional version of the HR model neurons. The model is comprised three dynamical variables comprising a fast subset,  $x(t)$  and  $y(t)$ , and a slower  $z(t)$ .  $x(t)$  represents the cell's membrane potential. These dynamical variables satisfy

$$\frac{dx(t)}{dt} = 4y(t) + 1.5x^2(t) - 0.25x^3(t) - 2z(t) + 2e + I_{syn} \quad (1)$$

$$\frac{dy(t)}{dt} = 0.5 - 0.625x^2(t) - y(t), \quad (2)$$

$$\frac{1}{\mu} \frac{dz(t)}{dt} = -z(t) + 2[x(t) + 3.2] \quad (3)$$

where  $e$  represents an injected DC current, and  $\mu$  is the parameter that controls the time constant of the slow variable. The parameters were chosen to place the isolated neurons in the chaotic spiking-bursting regime:  $e = 3.281$ ,  $\mu = 0.0021$ .

$I_{syn}$  represents the postsynaptic current evoked after the stimulation of a chemical graded synapse. In this paper we consider only inhibitory synapses, which is the main kind of interconnection present in the pyloric CPG of the lobster. The synaptic current has been simulated with the traditional description used in the dynamical clamp technique [Sharp et al 1993] with minor modifications:

$$I_{syn} = -gr(x_{pre})\vartheta(x_{post}) \quad (4)$$

where  $g$  is the maximal synaptic conductance, and  $x_{\text{post}}$  is the membrane potential of the postsynaptic neuron.  $r(x_{\text{pre}})$  is the synaptic activation variable determined from the presynaptic activity by:

$$\frac{dr}{dt} = [r_{\infty}(x_{\text{pre}}) - r]/\tau_r \quad (5)$$

$$r_{\infty}(x_{\text{pre}}) = [1 + \tanh((x_{\text{pre}} + A)/B)]/2. \quad (6)$$

In our work  $A = 1, 2$  and  $B = 0.9$ .  $\tau_r$  is the characteristic time constant of the synapse ( $\tau_r \sim 100$ ).

$\vartheta(x_{\text{post}})$  is a nonlinear function of the membrane potential of the postsynaptic neuron:

$$\vartheta(x_{\text{post}}) = (1 + \tanh((x_{\text{post}} + a)/b)). \quad (7)$$

$$(8)$$

The parameters for  $\vartheta(x_{\text{post}})$  ( $a = 2.807514$  and  $b = 0.4$  in this paper) were chosen so that this function remained linear for the slow oscillations, the subthreshold regions for the fast spikes:

$$\left. \frac{d\vartheta(x)}{dx} \right|_{a,b} \sim 1, \quad (9)$$

$$\left. \vartheta(x) \right|_{a,b} \sim 0. \quad (10)$$

Each pair of model neurons were connected in mutual inhibitory configurations consisting of basic two-cell units such as the one shown in Figure 2.

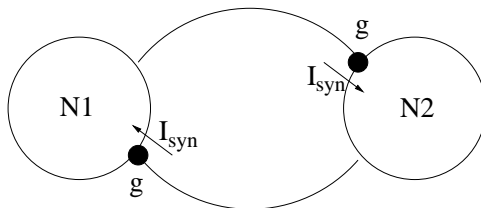


Figure 2: Basic configuration of synaptic couplings of the model for mutual inhibition between two neurons. The graded synapses are described by equations (4-8) in the text.

### 3 The models for the CPG and the mechanical device

We have previously built a CPG that controls a pyloric chamber model [Huerta et al, in press]. The CPG is composed of three neurons with mutual inhibitory coupling as shown in Fig. 2.

The configuration we selected is shown in Figure 3. The six independent maximal conductances  $g_{ij}$ ;  $i \neq j$ ;  $i, j = 1, 2, 3$  are to be selected as described below. The CPG sends electrical activity to the ‘muscles’ which control the dilation and contraction of the ‘pyloric chamber’ represented here by a simulated mechanical ‘plant’. Three neurons are the minimal number of neurons that produces a maximization of the average flow of food pumped out of the plant.

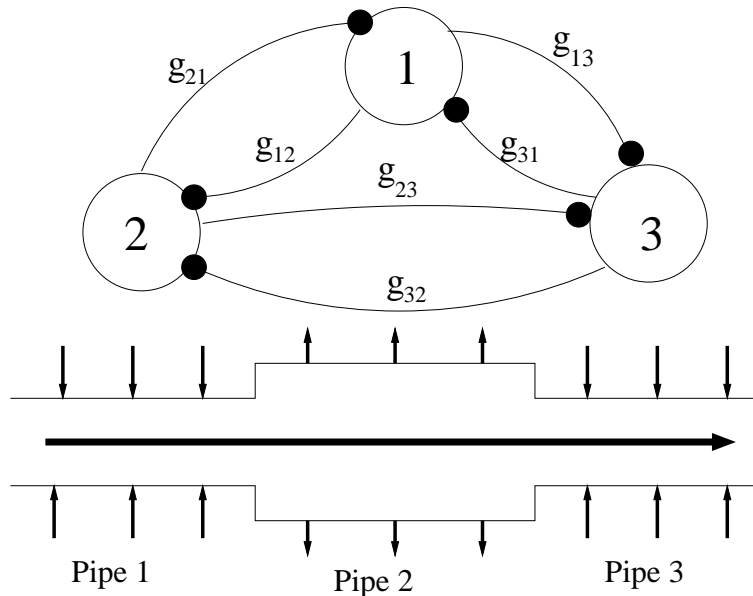


Figure 3: Illustration of the mechanical plant and the CPG. In the upper part of this figure we show the three neuron CPG and the six possible connections  $g_{ij}$  among them using mutual inhibition. In the lower half of the figure we show the pumping ‘plant’ composed of three pipes which can vary their radius. Each CPG neuron only affects one segment of the pipe. A detailed description of the pump is given in [Huerta et al, in press].

The mechanical plant is inspired by the lobster pyloric chamber [Selverston & Moulins 1987]. In Fig. 3 we have sketched the model with three joined pipes that can expand or contract radially. The central pipe only dilates and the end pipes only contract; this mimics the behavior of the pyloric chamber of the lobster. The proper dynamical combination of muscle activity influencing the walls of the pipes will lead to movement of shredded food towards the right end of the pyloric chamber.

In our selection procedure for combinations of the  $g_{ij}$ , we set the average transport through the pump in time  $T$  to a set of increasingly larger values and determine which configurations are able to achieve each level of transport. The average throughput over time  $T$  is given by

$$\Phi(g_{ij}) = \frac{\rho}{T} \int_{t_0}^{t_0+T} A_3(t)v_6(t)dt, \quad (11)$$

where  $\rho$  is the density of the material being pumped,  $A_3(t)$  is the cross sectional area of the rightmost pipe section,  $v_6(t)$  is the mean velocity through the rightmost cross section of the plant, and  $t_0$  is some starting time. The differential equations determining  $A_3(t)$  and  $v_6(t)$  were derived in [Huerta et al, in press]. They come from the Navier-Stokes equations and from mass and energy conservation. We treat the shredded food as homogeneous, incompressible and isothermal, and it moves with low Reynolds number so the flow is always laminar and all radial velocities in the pipe sections are small. We also assume that no food leaks out during the pumping and that there were no head-losses in the joints of the pipes.

In our calculations the mean initial velocities in the sections are zero. We choose a set of  $g_{ij}$  as indicated in a moment, and ask whether the specified configuration can achieve a chosen level of  $\Phi(g_{ij})$ . The system of differential equations was integrated using a Runge-Kutta 6(5) scheme with variable time step and with an absolute error of  $10^{-16}$  and a relative error of  $10^{-6}$ .

We choose the  $g_{ij}$  to be 0, 50nS, or 200nS, and evaluate  $\Phi(g_{ij})$  for each of these  $3^6$  choices. The system was run for a simulated time of 60 sec; a transient of  $t_0 = 10$  sec was eliminated and  $\Phi(g_{ij})$  was found by averaging over the last  $T = 50$  sec.

In the following section we will compare the performance of both regular and chaotic neurons in controlling the pump for the different connection architectures. The detailed description of the regular HH model can be found in [Huerta et al, in press]. The chaotic neurons were implemented as described in the previous section. Both types of neurons are able to generate spiking-bursting behavior.

## 4 Analysis of solutions

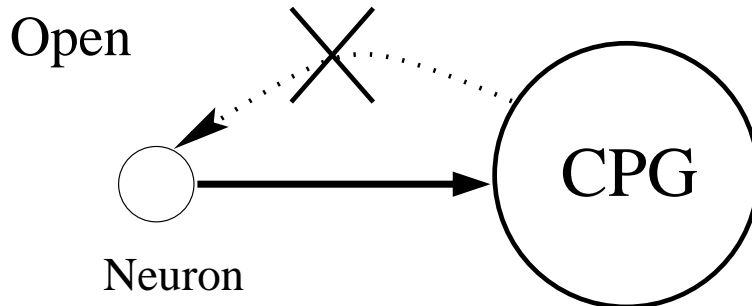


Figure 4: Definition of an **open** network topology: there must be one or more neuron without feedback from the remaining neurons.

It is useful to distinguish among three different types of topologies:

- **Open topology:** in this case there is one or more neuron which receives no feedback from the other network elements. This is shown in Figure 4.
- **Semi-open topology:** in this case there is one or more neuron which receives input from some neurons in the network, but no connection is made back to the network.
- **Closed topology:** in this case there are connections from each network member to and from the remainder of the network.

In order to quantify the difference between open topologies and the others we introduce the following definitions. We define the set of solutions with a resulting flow lying in  $\Phi_{lower} \leq \Phi \leq \Phi_{upper}$  as

$$G(\Phi_{lower}, \Phi_{upper}) = \{(g_{12}, g_{13}, g_{21}, g_{23}, g_{31}, g_{32}); \Phi_{lower} < \Phi \leq \Phi_{upper}\}. \quad (12)$$

and the subset of open solutions as

$$O(\Phi_{lower}, \Phi_{upper}) = \{(g_{12}, g_{13}, g_{21}, g_{23}, g_{31}, g_{32}); \exists i/g_{ji} = 0, \forall j \neq i; \Phi_{lower} < \Phi \leq \Phi_{upper}\}. \quad (13)$$

We report the ratio between the number of open solutions  $|O(\Phi_{lower}, \Phi_{upper})|$  and the total number of solutions  $|G(\Phi_{lower}, \Phi_{upper})|$

$$\eta(\Phi_{lower}, \Phi_{upper}) = \begin{cases} |O(\Phi_{lower}, \Phi_{upper})| / |G(\Phi_{lower}, \Phi_{upper})| & \text{if } |G(\Phi_{lower}, \Phi_{upper})| \neq 0 \\ 0 & \text{if } |G(\Phi_{lower}, \Phi_{upper})| = 0 \end{cases} \quad (14)$$

as a quantitative measure of the topology of allowed solutions at a given value of  $\Phi$ .  $|\dots|$  denotes the cardinality of a set. Since  $|O(\Phi_{lower}, \Phi_{upper})| \leq |G(\Phi_{lower}, \Phi_{upper})|$ ,  $0 \leq \eta \leq 1$ .

We investigated two questions in the calculations reported here:

- Does the use of chaotic component CPG neurons filter out open solutions ?
- Can noise eliminate open solutions when the component CPG neurons are regular oscillators?

In examining the first question we used three different values of the  $g_{ij}$  as indicated above for both the regular neuron model and the chaotic neuron model. The number of configurations was  $3^6$ . The number of simulation trials for a given configuration pattern was 15 for different random initial conditions. In Figure 5 we can see a plot of  $\eta(\Phi_{lower}, \Phi_{upper})$  as defined in Equation 14. We can see that as the flow  $\Phi$  increases there are no open topologies of chaotic component neurons

which can achieve the flow level.  $\Phi$  must be substantially reduced to find allowed open topology synaptic connection configurations.

If we build the CPG with regular neurons we see that there are many open topology solutions for high values of  $\Phi$ . Moreover, the  $\eta(\Phi)$  is strongly decreasing for the CPG with chaotic neurons. However, the intrinsically regular CPG does not lead to a strong dependence of  $\eta$  on the level of the flow.

This is one of the essential points of our work. Since the neurons in the pyloric CPG appear to oscillate chaotically, a closed topology of synaptic connections is required to achieve high transport rates for food. Regular neurons can achieve high transport rates in open and in closed configurations, but the pyloric CPG is observed to be closed. Our calculations provide a suggestive connection between these observations. CPGs made of chaotic neurons could have evolved open topologies, but these are not as effective in transporting food as closed topologies and presumably were not selected in evolutionary processes. This means that by means of chaotic neurons a selective choice of available solutions is obtained. Intrinsic chaotic dynamics in the isolated neurons provide a straightforward explanation of the existence of non-open connection topologies in invertebrate's CPGs.

To address our second question iid  $N(0,1)$  white noise  $\epsilon(t)$  is introduced in the external injected currents of the Hodgkin-Huxley model [Huerta et al, in press] so  $I(t) = I_o + \sigma\epsilon(t)$  where  $\sigma$  is the amplitude of the noise. We introduce this type of additive noise for simplicity, because it can be more easily integrated [Mannella & Palleschi] since there is no dependence on the other variables of the ordinary differential equations. In Figure 5 we can see the results of our calculations for 8 different values of  $\sigma$ . For each  $\sigma$  value 20 trials of different initial conditions for a given configuration of  $g_{ij}$  were carried out and the average of those values was taken as the output of the calculation. The quantity we used to estimate changes as a function of  $\sigma$  is

$$\eta(\sigma) = \begin{cases} |O_\sigma(\Phi_{th}, \Phi_{max})| / |G_\sigma(\Phi_{th}, \Phi_{max})|, & \text{if } |G_\sigma(\Phi_{th}, \Phi_{max})| \neq 0 \\ 0 & \text{if } |G_\sigma(\Phi_{th}, \Phi_{max})| = 0 \end{cases}$$

where  $\Phi_{max} = \max_{\mathbf{g}}\{\Phi\}$  and  $\Phi_{th}$  is the threshold value that determines the existence of good solutions. If a reduction in the number of open configurations is observed the value  $\eta(\sigma)$  must decrease. If our selected configurations are eliminated by noise, then open-topology configurations should disappear and  $\eta(\sigma)$  must tend to 0. Otherwise for any value of noise then  $\eta(\sigma)$  is always greater than 0. In fig 5 we can clearly see that for any value of the noise no reduction of the open-topology configurations is observed. Moreover, the quantity  $\eta$  approaches 1 for high values of the noise which answers our question about noise in the positive: the open configurations of

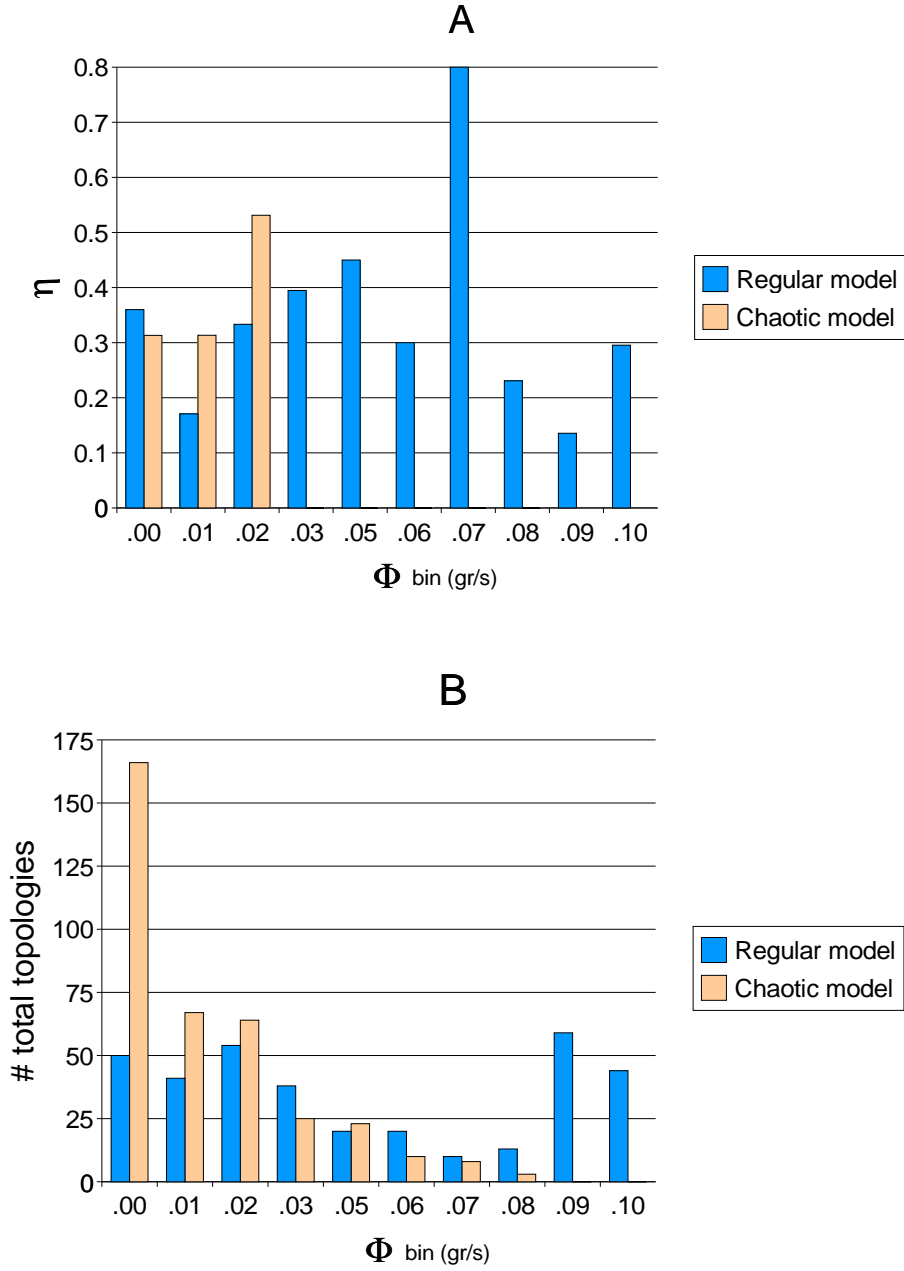


Figure 5: **A.**  $\eta(\Phi_{\text{lower}}, \Phi_{\text{upper}})$  for the regular and chaotic component CPGs. The data are presented by placing the average transport in bins defined by  $\Phi_{\text{lower}} = \Phi$  and  $\Phi_{\text{upper}} = 1.01\Phi$ . As we increase the transport level  $\Phi$ , the number of open solutions which can achieve this level goes rapidly to zero. **B.** Number of total allowed configurations for both the regular and chaotic CPG as a function of the level of average transport  $\Phi$ .

regular component CPGs are robust against the presence of synaptic noise. The appearance of closed configurations must have a different explanation, and that we have provided above.

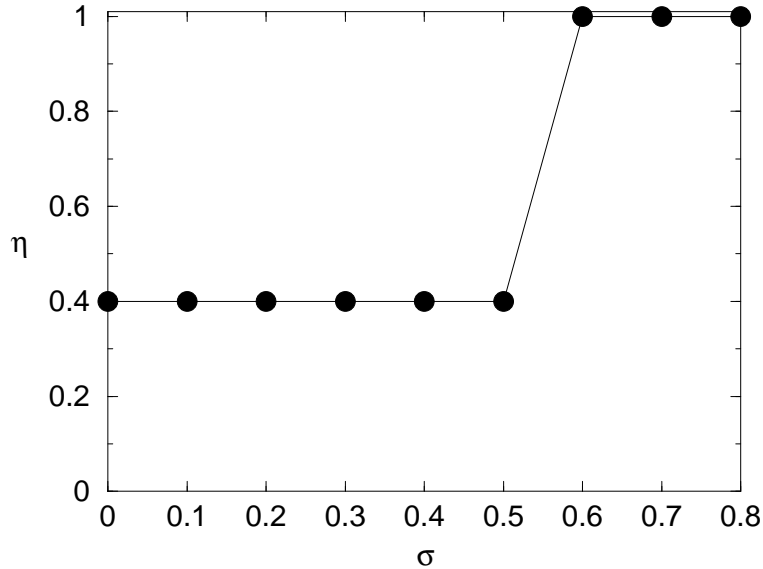


Figure 6:  $\eta(\sigma)$  for regular Hodgkin-Huxley neurons as CPG components. model. The open-topology configurations are not eliminated because of the noise. In these calculations  $\Phi = 0.06$  (gr/sec).

## 5 Conclusion

In this paper we have concentrated on the lobster pyloric CPG as we have experimental evidence of the chaotic oscillations of its component neurons when they are isolated from the intact network. There are many other invertebrate CPGs as shown in Figure 1, and a common thread among these CPGs, whether they are involved in shredding food, as in the gastric CPG of crustacea, feeding, as in the *Planorbis*, or swimming as in *Tritonia* is that the topology of the CPG network is closed. It would be very interesting to follow the path we have set out here for these and other CPGs to establish whether the connection between network topology , efficiency in biological function and chaotic neuronal elements holds there as well.

Since the early papers that showed evidence of chaos in CPG neurons [Hayashi & Ishizuka, 1992, Mpitsos et al 1988] little attention has been given to the role of chaotic neurons in CPGs. It appears that the main reason is that intact CPG networks work in a regular fashion. Indeed their task is to provide a regular rhythm to the animal so that the appropriate response of the muscles that operate in a physical device, such as the pyloric chamber, performs a specific function.

Therefore, the interest of modelers was focused mainly on studying the dynamics of periodic model neurons [Skinner et al 1993, Kepler et al 1990, Terman et al 1998, Baer et al 1995, Roberts 1998, Huerta 1996]. In very few cases modelers have tried to understand the potential advantages of using chaotic neurons [Freeman 1996, Rabinovich & Abarbanel 1998, Zak 1991], but typically in more complex systems, not in CPGs. By means of this work we hope to draw the reader's attention to an interesting set of roles played by chaotic neurons in CPGs.

The connectivity of neurons in CPGs is probably determined by many developmental and evolutionary factors, and in this paper we have considered an aspect of the required function of a CPG as providing a significant driving force in this topological decision. Starting from the observation that component neurons from the lobster pyloric CPG have chaotic membrane potential oscillations when observed in isolation [Abarbanel et al 1996], we have investigated the influence that chaotic versus regular neurons might have on the structure of the neural interconnections in the CPG in order to achieve its functional goal. If our conclusions are to extend to other CPGs, clearly one must systematically, as we have for the pyloric CPG of lobster, establish the modes of oscillation for the CPG members in isolation. We conjecture that the example of lobster pyloric CPG is not special, but we are seeing in this example a pattern which will repeat in other CPG systems.

## Acknowledgements

This work was supported in part by the U.S. Department of Energy, Office of Basic Energy Sciences, Division of Engineering and Geosciences, under grants DE-FG03-90ER14138 and DE-FG03-96ER14592. We thank Rob Elson, Allen Selverston, and Attila Szücs for many conversations about the material in this paper.

## References

- [Abarbanel et al 1996] Abarbanel H. D. I., Huerta R., Rabinovich, M. I., Rulkov, N. F., Rowat, P. F., Selverston A. I. (1996) Synchronized Action of Synaptically Coupled Chaotic Model Neurons. *Neural Computation* 8: 1567-1602.
- [Arshavsky et al 1985] Arshavsky, Y.I., Beloozerova I.N., Orlovsky, G.N., Panchin & Y.V., Pavlova, G.A. Control of locomotion in marine mollusc *Clione limacina*. *Exp Brain Res* 58, 255-293 (1985).
- [Arshavsky et al 1991] Arshavsky, Y.I., Grillner, S., Orlovsky, G.N., & Panchin, Y.V. Central generators and the spatiotemporal pattern of movements. In: *The Development of Timing Control* (Fagard J., Wolff P.H., eds.), 93-115. (Elsevier. Amsterdam. 1991).
- [Bazhenov et al 1998] Bazhenov, M., Huerta, R., Rabinovich, M.I. and Sejnowski, T. Cooperative behavior of a chain of synaptically coupled chaotic neurons. *Physica D*, vol.116, (no.3-4), Elsevier, 1 June 1998. p.392-400
- [Elson et al 1999] Elson, R. C., Huerta, R. Abarbanel, H. D. I. Rabinovich, M.I. & Selverston, A. I. Dynamic Control of Irregular Bursting in an Identified Neuron of an Oscillatory Circuit. *J. Neurophysiology* 82, 115-122 (1999).
- [Elson et al 1998] Elson, R. C., Maher, M, Abarbanel H. D. I., Rabinovich M. I., Selverston A. I. (1998) Synchronization and Regularization Phenomena in Coupled Irregularly Bursting Neurons: I. Experimental Studies. In "From Physics to Biology". Kluwer Academic Publishers.
- [Freeman 1996] Freeman, W. J. Random activity at the microscopic neural level in cortex ("noise") sustains and is regulated by low-dimensional dynamics of macroscopic cortical activity ("chaos"). *International Journal of Neural Systems*, 7(4):473-80 (1996).
- [Getting 1989] Getting, P.A. Emerging principles governing the operation of neural networks. *Ann Rev Neurosci.*, 12, 185-204, (1989).
- [Hayashi & Ishizuka, 1992] Hayashi, H. & Ishizuka, S. Chaotic nature of bursting discharges on *Oncidium* pacemaker neuron. *J. Theor. Biol.* 156, 269-291, (1992).
- [Hindmarsh & Rose, 1984] Hindmarsh, J.L. & Rose, R.M. A model of neuronal bursting using three coupled first order differential equations. *Proc R. Soc. Lond. B* 221, 87-102 (1984).
- [Hodgkin & Huxley, 1952] Hodgkin, A. L. and A. F. Huxley, "A quantitative description of membrane current and its application to conduction and excitation in nerve", *Journal of Physiology*, 117, 500-544 (1952).
- [Huerta 1996] Huerta, R. A finite automata model of spiking-bursting neurons. *Int. J. Bifurcation and Chaos* 6: 705-714 (1996).
- [Huerta et al, in press] Huerta, H., Sanchez-Montañes, M. A., Corbacho, F., and Siguenza, J. A., *Biological Cybernetics* (in press).
- [Kepler et al 1990] Kepler, T.B., E. Marder, E. & Abbott, L.F. . The Effect of Electrical Coupling on the Frequency of Model Neuronal Oscillators. *Science* 248(4951), 83-85 (1990).
- [Mannella & Palleschi] Mannella, R. & Palleschi, V. Fast and precise algorithm for computer simulation of stochastic differential equations. *Physical Review A* 40(6), 3381-3386 (1989).
- [Marder & Calabrese 1996] Marder, E., Calabrese R. L. 1996. Principles of rhythmic motor pattern generation. *Physiol. Rev.* 76, 687-717.
- [Mpitsos et al 1988] Mpitsos, G.J., Burton, R.M., Creech, H.C. & Sojnila, S.O. Evidence for chaos in spike trains of neurons that generate rhythmic motor patterns. *Brain Research Bulletin*, 21(3):529-38, (1988).
- [Rabinovich & Abarbanel 1998] Rabinovich M. I. and Abarbanel H. D. I. (1998) The role of chaos in neural systems. *Neuroscience*, 87(1):5-14.
- [Baer et al 1995] Baer, S.M., Rinzler, J., & Carrillo, H. Analysis of an autonomous phase model for neuronal parabolic bursting. *Journal of Mathematical Biology*, vol.33, (no.3), 309-33 (1995).

- [Roberts 1998] Roberts P. D. (1998) Classification of temporal patterns in dynamic biological networks. *Neural Computation* 10: (7) 1831-1846.
- [Selverston & Moulins 1987] Selverston, A. I. & Moulins, M., eds. (1987). *The Crustacean Stomatogastric System* (Springer, Berlin, 1987).
- [Skinner et al 1993] F. K. Skinner, G.G. Turrigiano & E. Marder, Frequency and burst duration in oscillating neurons and two-cell networks. *Biological Cybernetics* 69, 375-383 (1993).
- [Sharp et al 1993] Sharp, A.A., O'Neil, M.B., Abbott, L.F., & Marder E. Dynamic Clamp: Computer-Generated Conductances in Real Neurons. *J. Neurophysiol.* 69, 3 (1993).
- [Szucs et al 1999] Szucs, A., Varona, P., Volkovskii, A., Abarbanel, H. D. I., Rabinovich, M. I., & Selverston, A. I. (1999). Interacting biological and electronic neurons produce realistic oscillatory rhythms. Submitted to Neuroreport.
- [Terman et al 1998] Terman, D., Kopell N., & Bose, A. Dynamics of two mutually coupled slow inhibitory neurons. *Physica D* 117, 241-275 (1998).
- [Wang 1993] Wang XJ (1993) Genesis of bursting oscillations in the Hindmarsh-Rose model and homoclinicity to a chaotic saddle. *Physica D* 62: 263-274.
- [Zak 1991] Zak, M. (1991) Terminal chaos for information processing in neurodynamics. *Biological Cybernetics*, 64(4):343-51.